3 1176 00148 2125

NACA RM L9E10

NACA

RESEARCH MEMORANDUM

EFFECTS OF MACH NUMBER AND SWEEP ON THE DAMPING-IN-ROLL

CHARACTERISTICS OF WINGS OF ASPECT RATIO 4

By

Richard E. Kuhn and Boyd C. Myers, II

Langley Aeronautical Laboratory
Langley Air Force Base, Va.

NATIONAL ADVISORY COMMITTEE
FOR AERONAUTICS

WASHINGTON

June 27, 1949

CONFIDENTIAL

UNCLASSIFIED

NATIONAL ADVISORY COMMITTEE FOR AERONAUTICS

RESEARCH MEMORANDUM

EFFECTS OF MACH NUMBER AND SWEEP ON THE DAMPING-IN-ROLL

CHARACTERISTICS OF WINGS OF ASPECT RATIO 4

By Richard E. Kuhn and Boyd C. Myers, II

SUMMARY

The damping-in-roll characteristics of three wings with an aspect ratio of 4, a taper ratio of 0.6, sweep angles of 3.6°, 32.6°, and 46.7° at the quarter-chord line, and with the NACA 65A006 section have been determined through the Mach number range from 0.4 to 0.91 and angle-of-attack range from 0° to 6.5° in the Langley high-speed 7- by 10-foot tunnel by the free-roll method. The results indicated that the increase in magnitude of the damping-in-roll coefficient C_{l_p} with Mach number and the decrease with sweep angle, at low angles of attack, agreed well with the theoretical variations. The damping coefficient increased markedly with angle of attack (in the test range) particularly at the higher Mach numbers investigated.

INTRODUCTION

Low-speed experimental data and theory (references 1 and 2) indicate an appreciable reduction in the damping-in-roll properties of a wing as the sweep angle is increased. The theoretical manner in which these effects are affected by compressibility is treated in references 2 and 3. Little experimental data, however, are available at high-subsonic Mach numbers for comparison with theory. Accordingly, an extensive investigation is being conducted in the Langley high-speed 7- by 10-foot tunnel to determine the effects of sweep angle and Mach number on the damping-in-roll characteristics of a series of wings. The first wing investigated was a 35° sweptback wing of aspect ratio 3, and the damping-in-roll characteristics of this wing at high-subsonic Mach numbers are presented in reference 4.

The present paper presents the results of an experimental determination of the damping-in-roll characteristics of three wings of aspect ratio 4 and taper ratio 0.6 with sweep angles of 3.6°, 32.6°, and 46.7° referred to the quarter-chord line. The investigation utilized the free-roll technique described in reference 4, and the tests were made at angles of attack of 0.30°, 3.45°, and 6.5° through a Mach number

range from 0.40 to 0.91. This paper also includes a comparison with
theoretical results computed from Weissinger's theory as presented in
reference 2 and from the more approximate, but more convenient, theory
of reference 3.

COEFFICIENTS AND SYMBOLS

A   wing aspect ratio

a   speed of sound, feet per second

b   wing span, (3.000 ft on model)

c'   mean aerodynamic chord (M.A.C.; 0.765 ft on model)

C_l rolling-moment coefficient (L/qSb)

C_{l_p} coefficient of damping in roll $\left(\dfrac{\partial C_l}{\partial \left(\frac{pb}{2V}\right)}\right)$

L   rolling moment, ft-lb

M   free-stream Mach number (V/a)

p   rate of roll, radians per second

q   dynamic pressure, pounds per square foot $\left(\rho V^2/2\right)$

$\Lambda_{c/4}$ sweep angle, degrees (referred to 25 percent chord)

R   Reynolds number $(\rho V c'/\mu)$

S   wing area (2.25 sq ft on model)

V   free-stream velocity, feet per second

ρ mass density of air, slugs per cubic foot

μ absolute viscosity, pound-seconds per square foot

α angle of attack of wing, degrees

δ control-surface deflection with reference to wing chord line
        parallel to plane of symmetry, degrees

ϵ angle of attack of wing-tip chord relative to root chord, radians

$pb/2V$ wing-tip helix angle, radians

$$C_{l_\delta} = \frac{\partial C_l}{\partial \delta}$$

$$\left(\frac{pb}{2V}\right)_\delta = \frac{\partial \left(\frac{pb}{2V}\right)}{\partial \delta}$$

K correction factor for wing distortion due to bending

Subscripts:

a_l left aileron

a_r right aileron

test   measured values, uncorrected for distortion due to bending

MODEL AND APPARATUS

The pertinent dimensions of the three wings used in the present investigation are given in figure 1. The wings were constructed of an aluminum alloy. The sweptback wings were designed by shearing the unswept wing; that is, the chordwise elements of the unswept wing parallel to the plane of symmetry were moved rearward until the desired sweep angle of the 25-percent-chord line was obtained. Thus, all wing sections parallel to the plane of symmetry are NACA 65A006 sections. The ailerons were true-contour, sealed-gap, plan flaps of 20 percent chord and 40 percent span.

The wings were supported by a sting extending forward into the test section from a vertical strut located behind the model. The vertical strut was part of the wind-tunnel balance system and both the strut and a portion of the sting were shielded from the air stream by a fairing. A schematic drawing of the support system and rolling apparatus is shown in figure 2. The angle of attack of the model was changed by varying the angle of incidence of the wing relative to the sting. This was accomplished by utilizing various incidence blocks fitted into the sting. A photograph of the installation is shown in figure 3. The rolling-moment data were obtained from wind-tunnel balance measurements with the sting restrained in roll. When the model was permitted to

roll freely under the moment created by the deflected ailerons, the
rate of roll was recorded electrically.

TESTS AND PROCEDURE

Scope

For each wing, static rolling-moment data and rates of roll were
obtained through a Mach number range of 0.4 to 0.91 at angles of attack
of 0.30°, 3.45°, and 6.50° and for aileron deflections of 0°, $\pm 4^\circ$,
and $\pm 8^\circ$ in a plane parallel to the plane of symmetry. The ailerons
were deflected oppositely so that the total differential aileron
deflections used were 0°, 8°, and 16°.

The size of the model used in the present investigation resulted
in an estimated choking Mach number of 0.94, and the data are believed
to be reliable to a corrected Mach number of about 0.91. The variation
of test Reynolds number with Mach number for average test conditions is
presented in figure 4.

Corrections

A small tare correction in the form of bearing friction was deter-
mined by forced rotation of the rolling apparatus, under both vertical
and horizontal loads, for the range of angular velocities encountered
in the tests. This bearing friction has been applied to the results in
the form of an increment of damping-in-roll coefficient equal to a
value of $C_{l_p} = -0.005$.

The rolling moment and Mach numbers have been corrected for blocking
by the model and its wake by the method of reference 5. The jet-boundary
effects were estimated and found to be negligible.

The aluminum-alloy wings were known to bend under load. Accordingly,
the effect of wing distortion on the test results was investigated. The
possible sources of error considered were: (1) deflection of the
ailerons under load; (2) twist of the wing about its elastic axis due
to the aerodynamic forces being applied at some distance from the
elastic axis; and, (3) the spanwise change in angle of attack due to
bending of the wing panel under the span-load distribution. The error
due to this last consideration is essentially zero, of course, for an
unswept wing but increases very markedly as the sweep angle is increased.

Static loading of the ailerons and calculations of the twist of the wing indicated that errors arising from points (1) and (2) are negligible; however, calculations of the maximum change in angle of attack of the wing tip of the sweptback wings due to bending of the wing panel indicate an appreciable change in the angle. This change in angle of attack is in such a direction as to reduce the rolling moment which is being produced by the ailerons and is only important when the model is restrained in roll for the static tests. When the model has attained a steady rate of roll, in the free-roll tests, the damping moment of the wing balances the aileron rolling moment. In this condition the lateral center of pressure for the damping moment and the aileron load are at slightly different spanwise locations, and there is some slight distortion of the wing. This distortion is negligible, however, when compared with the distortions in the restrained condition and the wing can be considered essentially rigid during the free-roll tests.

The rolling moment L_{test} which is measured during the static test is

$$L_{test} = L_\delta \delta - L_\epsilon \tag{1}$$

where L_ϵ is the rolling moment lost due to the bending of the wing. This increment of rolling moment L_ϵ can be estimated by the relation

$$L_\epsilon = C_{l_p} \epsilon qSb \tag{2}$$

where C_{l_p} is the damping coefficient for the rigid wing. This estimation involves the assumption that the angle of attack due to distortion varies linearly from zero at the root to ϵ at the tip. This is not strictly correct of course, but the assumption is believed to give a good first approximation of the increment of rolling moment lost due to bending.

In order to determine ϵ, the applied rolling moments L_{test} were approximated by concentrated loads applied to the wing at the center of load calculated on the basis of unswept-wing theory (reference 6). The change in angle of attack at the wing tip ϵ was measured relative to the root chord and the rate of change with rolling moment $\Delta\epsilon/\Delta L_{test}$ was determined.

Equation (2) can be written

$$L_\epsilon = C_{l_p} \frac{\Delta\epsilon}{\Delta L_{test}} L_{test} qSb \tag{3}$$

Substituting in equation (1) and dividing through by qSb gives

$$C_{l_{\delta_{test}}}\delta = C_{l_\delta}\delta - C_{l_{\delta_{test}}}\delta\left(C_{l_p}\frac{\Delta\epsilon}{\Delta L}qSb\right) \tag{4}$$

Dividing through by δ and transposing terms gives

$$C_{l_\delta} = C_{l_{\delta_{test}}}\left[1 + C_{l_p}\left(\frac{\Delta\epsilon}{\Delta L}\right)qSb\right] \tag{5}$$

or

$$C_{l_\delta} = K C_{l_{\delta_{test}}} \tag{6}$$

where

$$K = 1 + C_{l_p}\left(\frac{\Delta\epsilon}{\Delta L}\right)qSb \tag{7}$$

Equation (7) involves the use of the C_{l_p} for the rigid wing which has not been determined. However, a first approximation of C_{l_p} can be obtained by

$$C_{l_{p_{test}}} = -\frac{C_{l_{\delta_{test}}}}{\left(\frac{pb}{2V}\right)_\delta}$$

By using this value of $C_{l_{p_{test}}}$ in equations (7) and (6) a first approximation of K and C_{l_δ} can be obtained. With this value of C_{l_δ}, a second approximation of C_{l_p} is found and thus, by successive approximations, the final value of K was determined (fig. 5).

Reduction of Data

By use of the correction factor K developed in the previous section, the aileron-effectiveness parameter C_{l_δ} and the coefficient of damping in roll C_{l_p} were evaluated as follows:

$$C_{l_\delta} = KC_{l_{\delta_{test}}}$$

and

$$C_{l_p} = \frac{\partial C_l}{\partial \left(\frac{pb}{2V}\right)} = -\frac{C_{l_\delta}}{\left(\frac{pb}{2V}\right)_\delta}$$

where the expressions $C_{l_{\delta_{test}}}$ and $(pb/2V)_\delta$ were evaluated graphically as the slopes of the static rolling-moment coefficient C_l plotted against aileron deflection δ and the nondimensional steady rate of rolling $pb/2V$ plotted against aileron deflection δ, respectively. This method of determining C_{l_p} assumes that the effects of rolling on C_{l_δ} are negligible (except for distortion corrections previously discussed) and that C_{l_p} is independent of aileron deflection.

RESULTS AND DISCUSSION

The results of the investigation are presented in the following figures:

The experimental variation of the damping-in-roll parameter C_{l_p} with Mach number at low angles of attack (figs. 12 to 14) shows an increase in magnitude of C_{l_p} with increasing Mach number for all three wings and agrees well with the theoretical variation according to reference 2. However, the theory slightly underestimates the absolute magnitude of the damping coefficient throughout the range. The theoretical variation according to reference 3 (based on the C_{l_p} at zero Mach number from reference 2) predicts the absolute values fairly well but shows a greater variation with Mach number.

Cross plots of the test data against sweep at several Mach numbers (fig. 15) indicate an appreciable reduction in the damping coefficient C_{l_p} with increasing sweep angle and compares very well with the theoretical variation (reference 2) at low angles of attack.

It will be noted that for the range tested C_{l_p} increases
appreciably with angle of attack, particularly at the higher Mach numbers.
A similar effect was noted in reference 4. The linearized theory, how-
ever, does not predict any variation of C_{l_p} with angle of attack
because it is evaluated in terms of lift rather than resultant force and
does not consider any nonlinear variation of lift with angle of attack.
The section data for these wings are not available but a value of 2π
was assumed for the lift-curve slope in the theoretical calculations.
A study of the effect of nonlinear lift characteristics has been made
in reference 7 and has indicated that this effect alone can cause large
changes in C_{l_p}.

CONCLUSIONS

On the basis of an investigation of the damping characteristics of
three wings of aspect ratio 4 and taper ratio 0.6 having quarter-chord
line sweep angles of 3.6°, 32.6°, and 46.7° in the Mach number range
from 0.40 to 0.91, the following conclusions can be drawn:

1. The damping-in-roll coefficient C_{l_p} increased in magnitude
with Mach number and decreased with sweep angle at low angles of attack
(0.30° and 3.45°) in the same manner as that predicted by theory.

2. The magnitude of the damping-in-roll coefficient C_{l_p} increased
markedly with angle of attack (in the test range from 0.30° to 6.5°)
particularly at the higher Mach numbers.

Langley Aeronautical Laboratory
        National Advisory Committee for Aeronautics
                Langley Air Force Base, Va.

REFERENCES

1. Toll, Thomas A., and Queijo, M. J.: Approximate Relations and Charts for Low-Speed Stability Derivatives of Swept Wings. NACA TN 1581, 1948.

2. Bird, John D.: Some Theoretical Low-Speed Span Loading Characteristics of Swept Wings in Roll and Sideslip. NACA TN 1839, 1949.

3. Fisher, Lewis R.: Approximate Corrections for the Effects of Compressibility on the Subsonic Stability Derivatives of Swept Wings. NACA TN 1854, 1949.

4. Myers, Boyd C., II, and Kuhn, Richard E.: High-Subsonic Damping-in-Roll Characteristics of a Wing with the Quarter-Chord Line Swept Back 35° and with Aspect Ratio 3 and Taper Ratio 0.6. NACA RM L9C23, 1949.

5. Herriot, John G.: Blockage Corrections for Three-Dimensional-Flow Closed-Throat Wind Tunnels, with Consideration of the Effect of Compressibility. NACA RM A7B28, 1947.

6. Pearson, Henry A., and Jones, Robert T.: Theoretical Stability and Control Characteristics of Wings with Various Amounts of Taper and Twist. NACA Rep. 635, 1938.

7. MacLachlan, Robert, and Letko, William: Correlation of Two Experimental Methods of Determining the Rolling Characteristics of Unswept Wings. NACA TN 1309, 1947.

▬▬▬▬

Figure 1.— A drawing of the three wings tested in the present investigation.
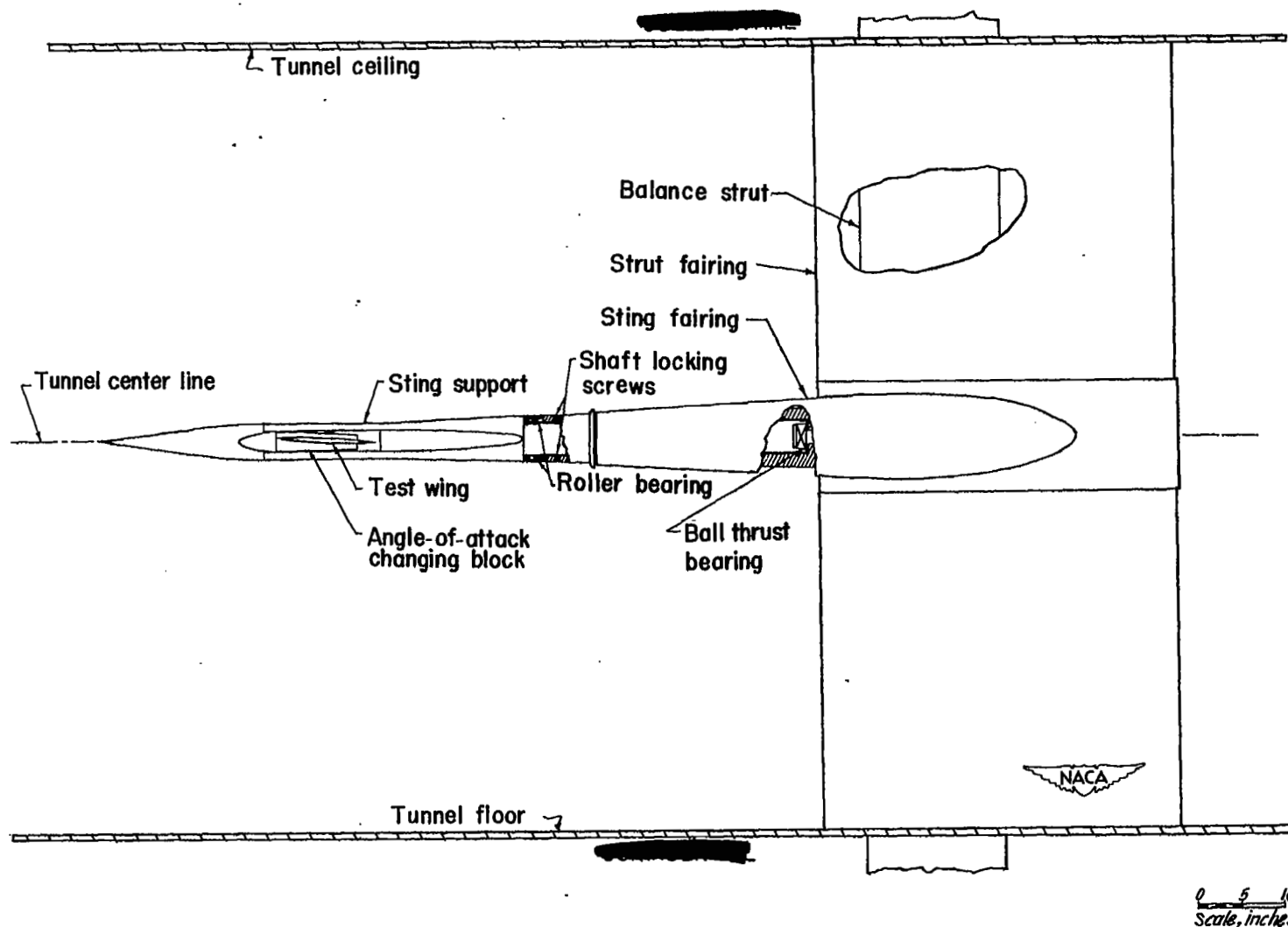
Figure 2.— Schematic drawing of the free—rolling sting mounted in the Langley high—speed 7— by 10—foot—tunnel test section.
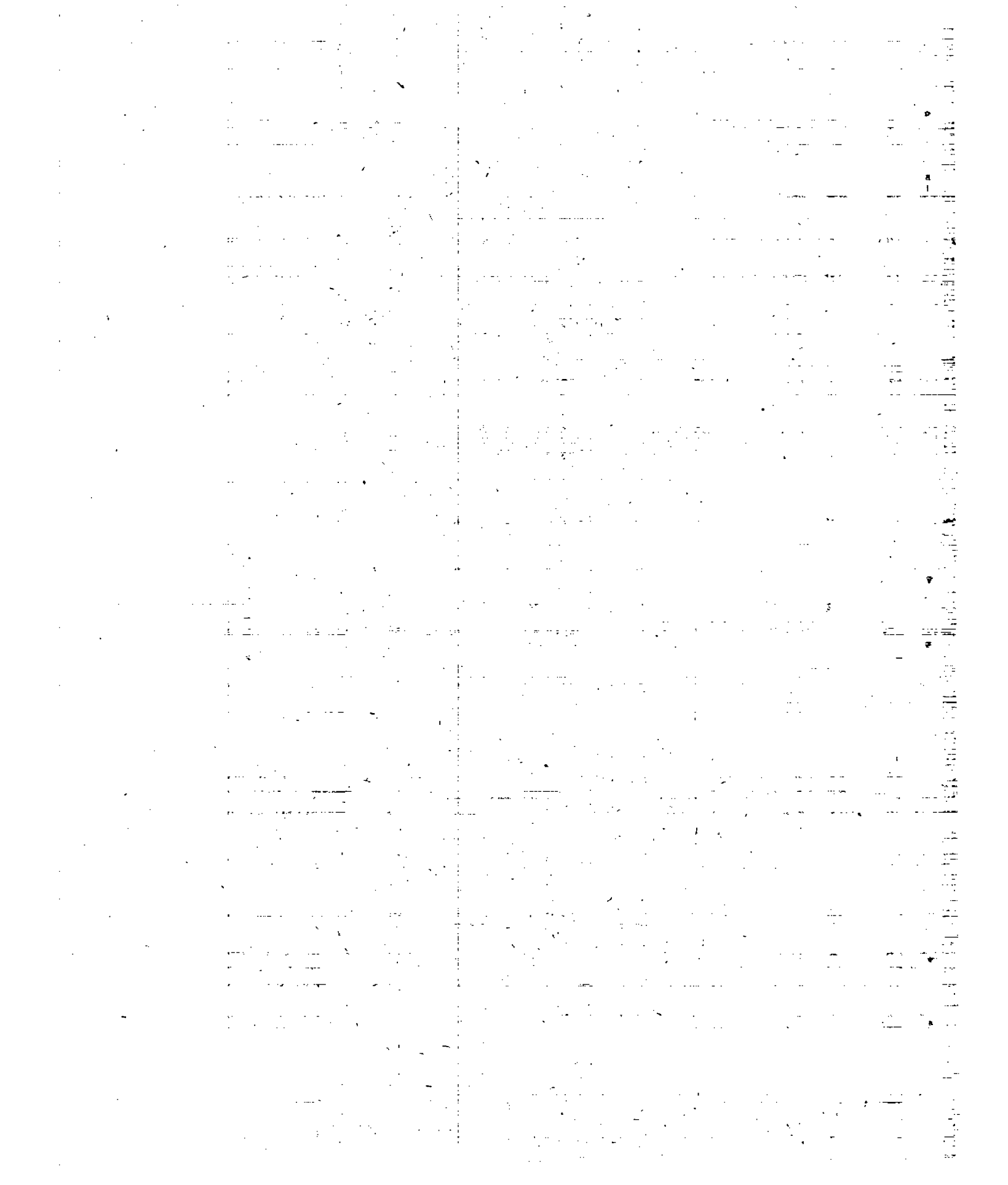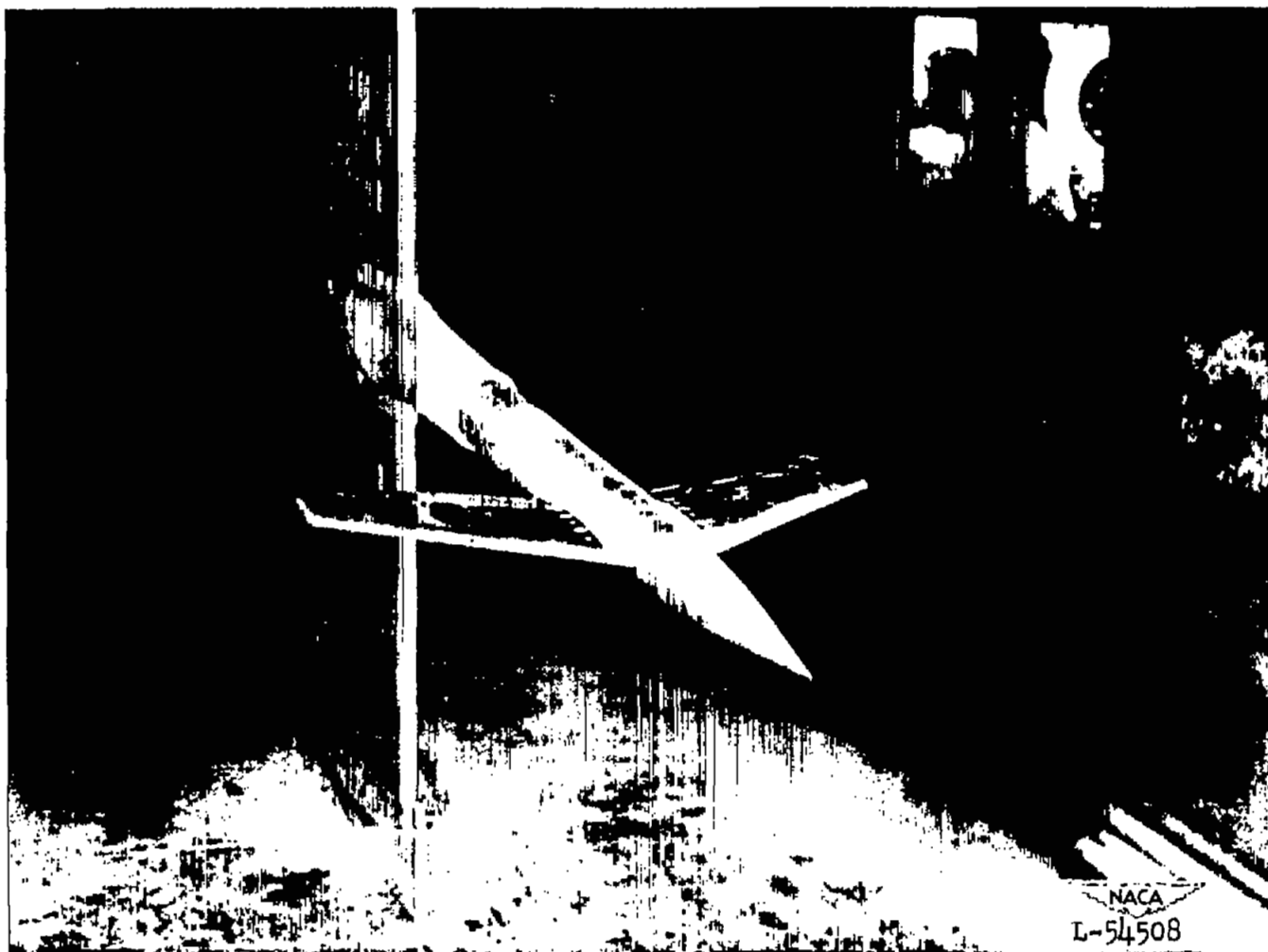
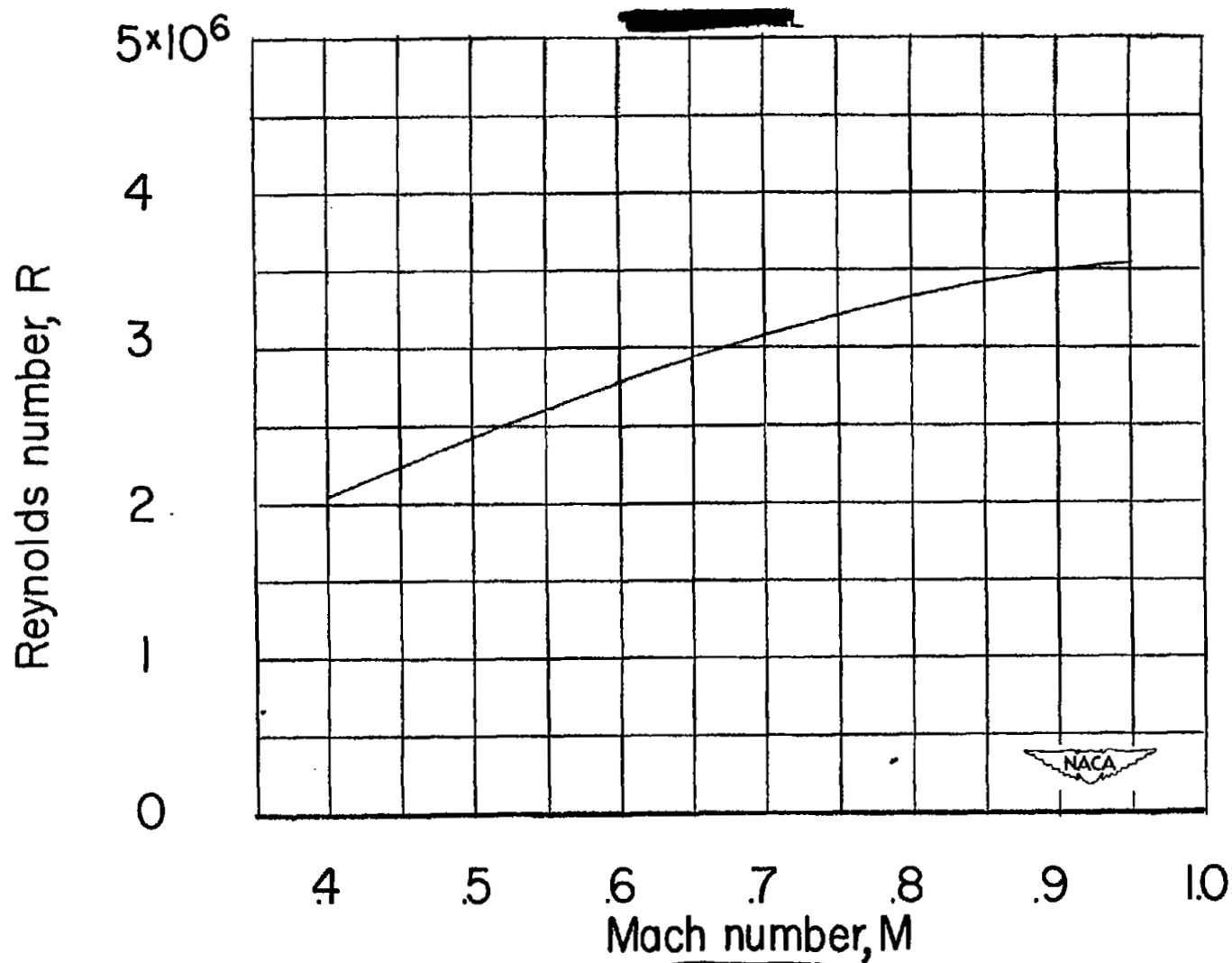Figure 3.— Test wing mounted on the free-roll sting in the Langley high-speed 7- by 10-foot tunnel.
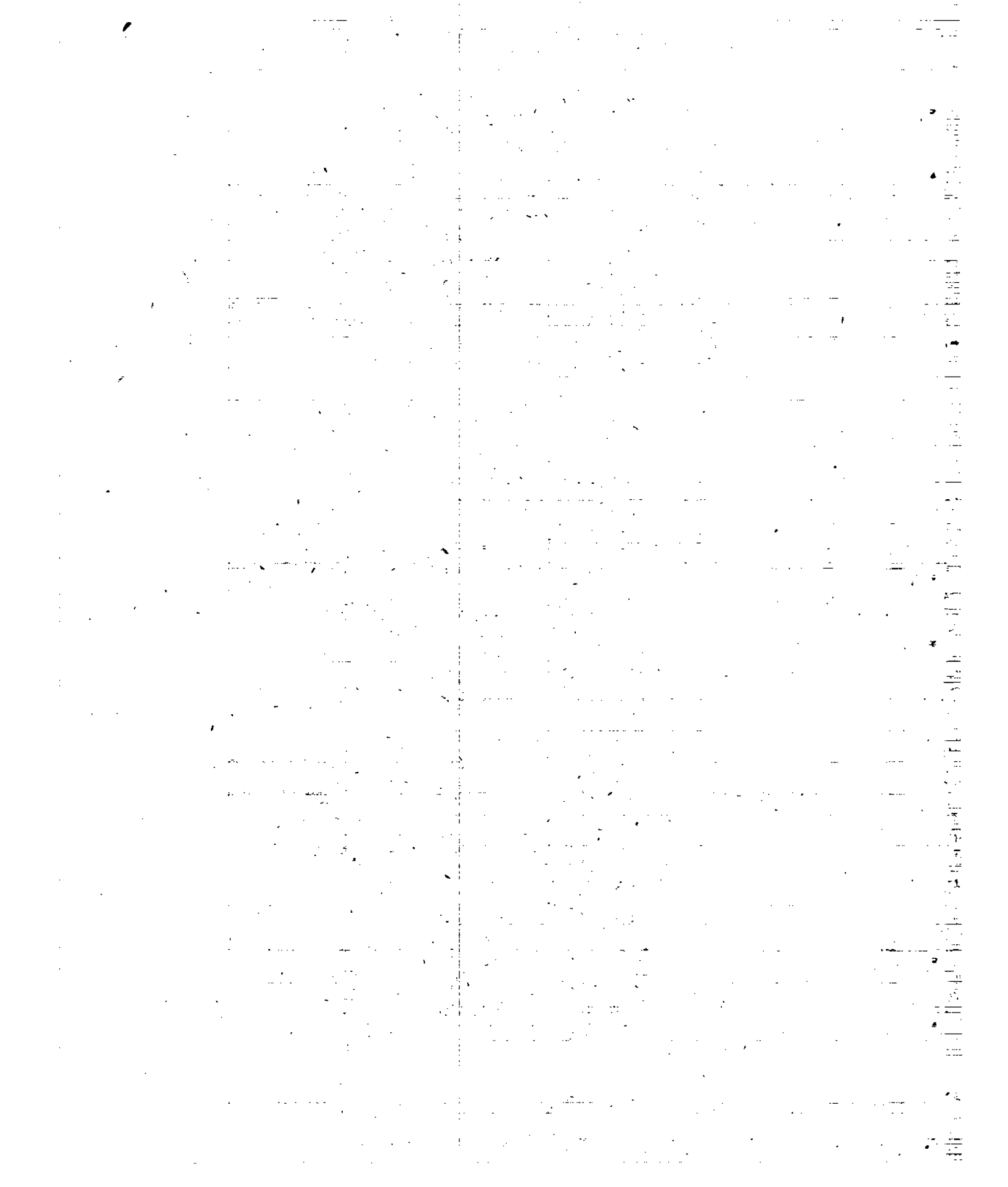
Figure 4.— The variation of test Reynolds number with Mach number based on the mean aerodynamic chord of 0.765 foot.
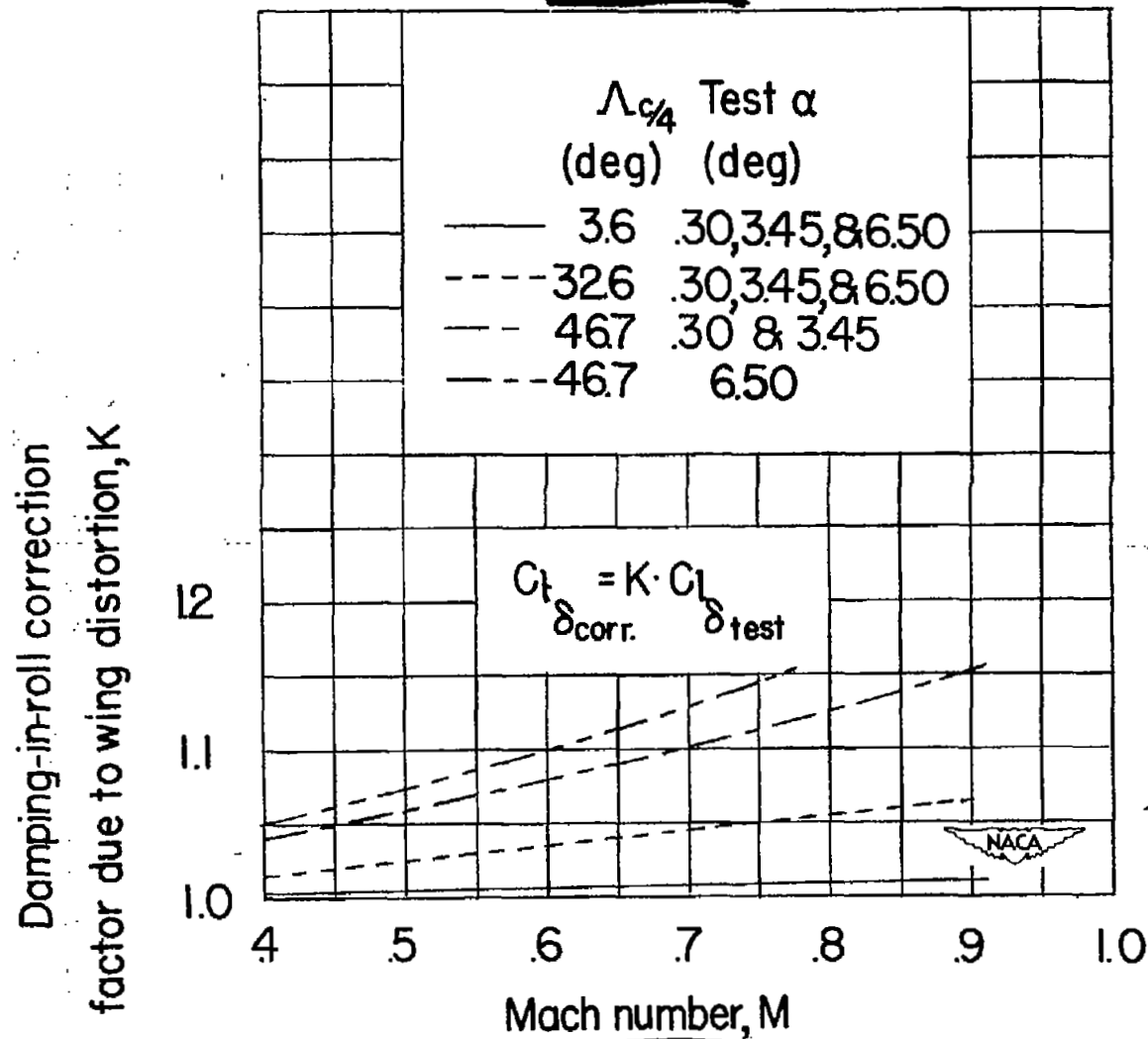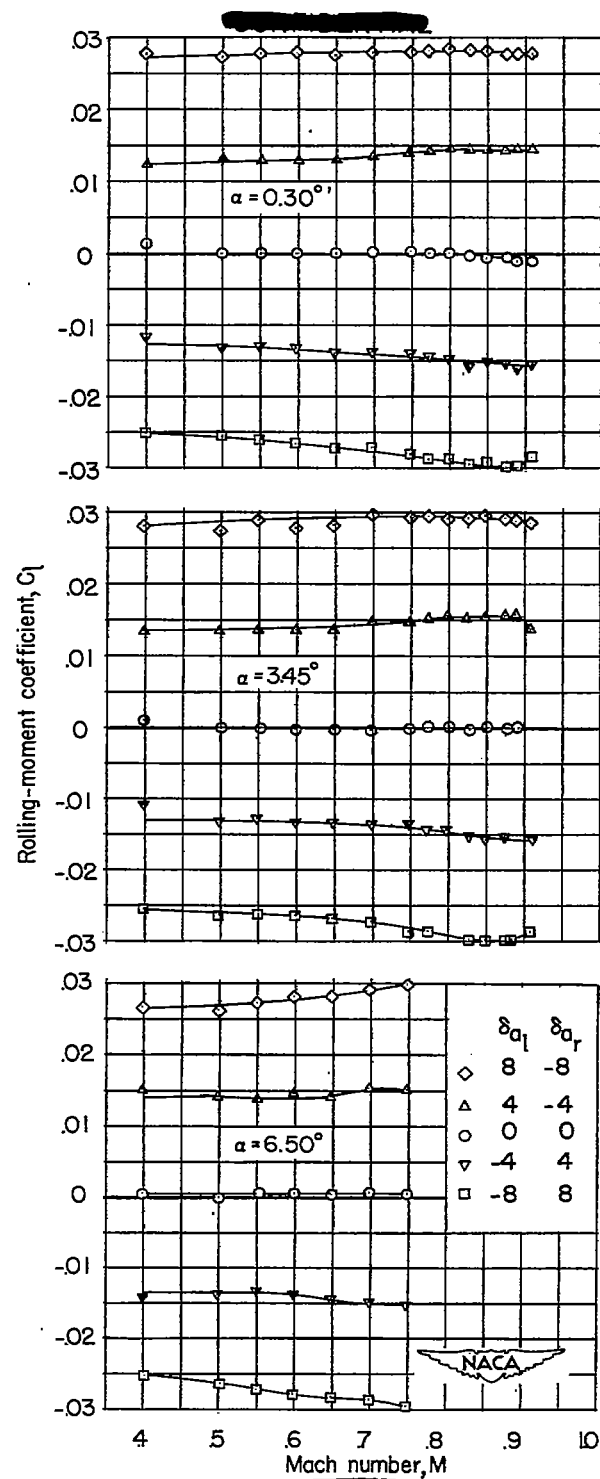
Figure 5.— Correction factor for elastic distortion of test wings under load.

Figure 6.— The variation with Mach number of the rolling-moment
characteristics of a wing for various aileron deflections at
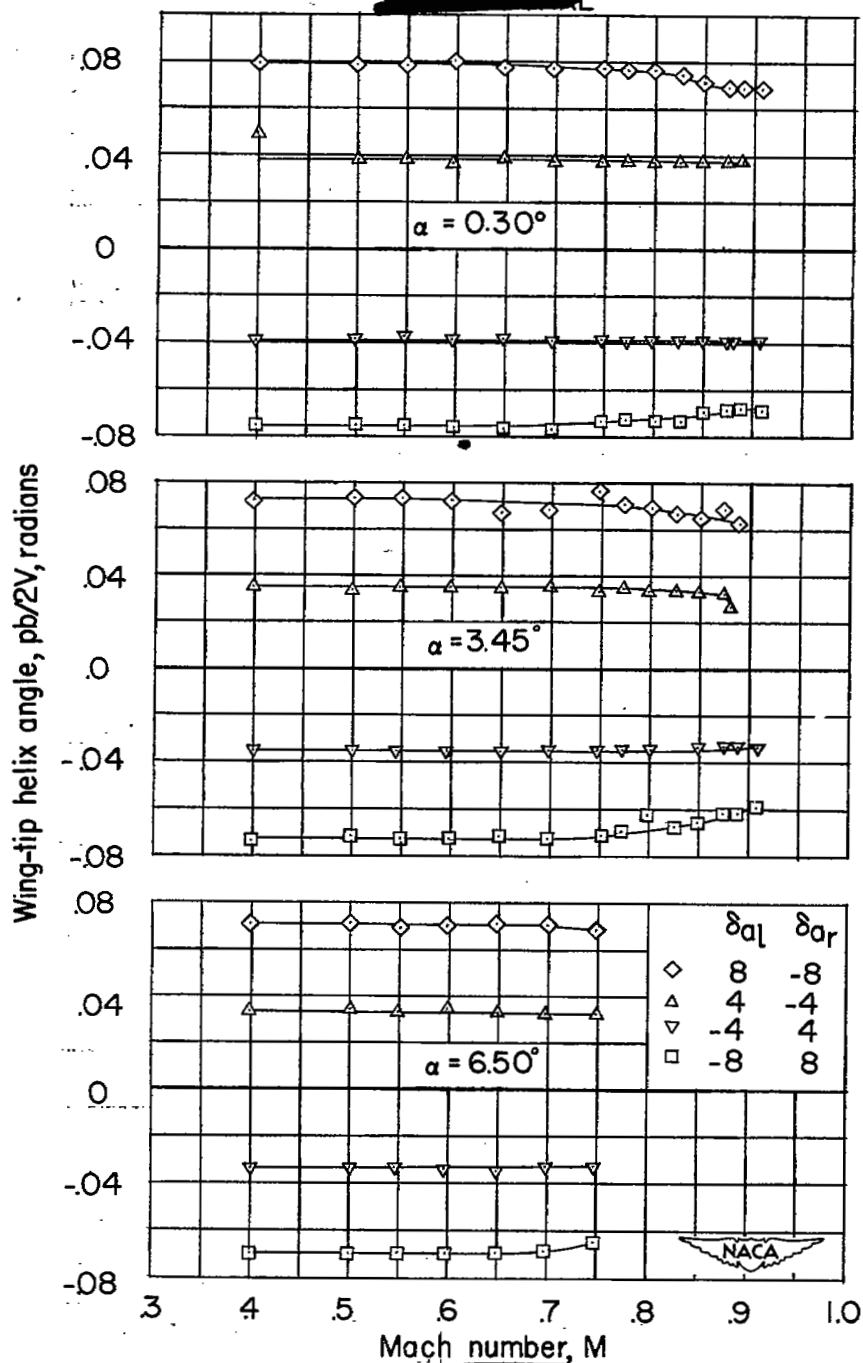several angles of attack. $\Lambda_{c/4} = 3.6^\circ$.
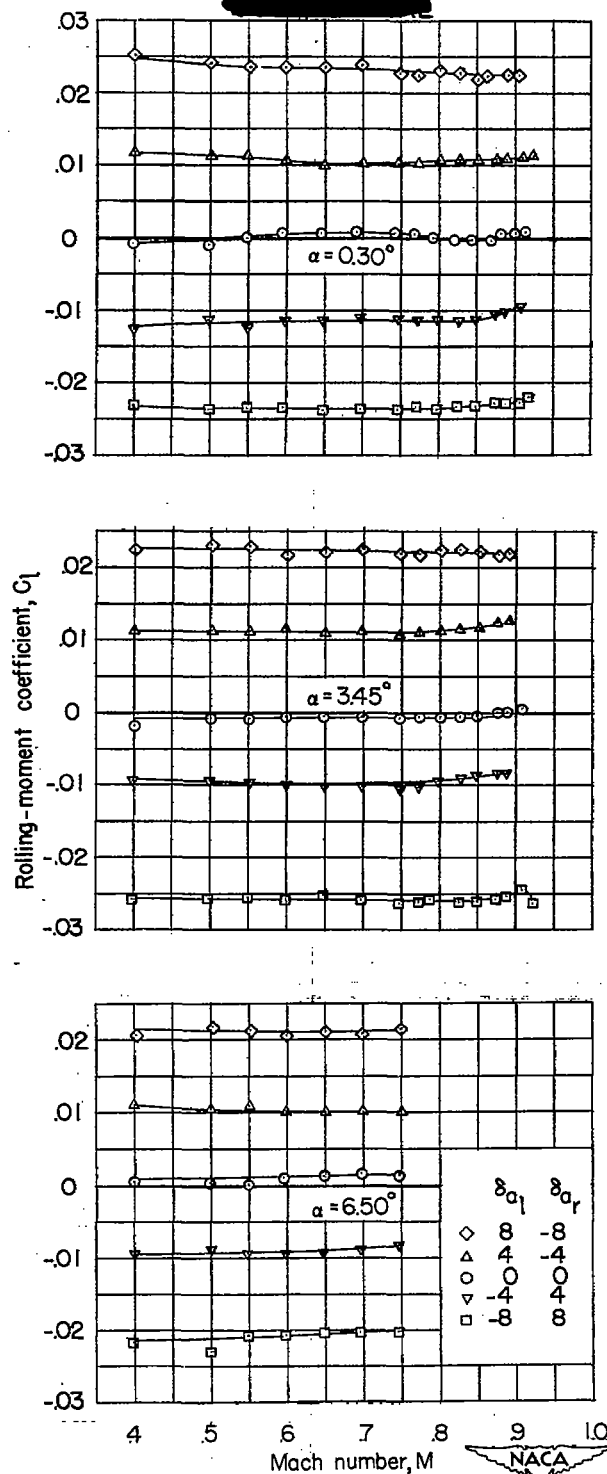
Figure 7.— The variation with Mach number of the rolling-moment characteristics of a wing for various aileron deflections at several angles of attack. $\Lambda_c/4 = 32.6°$.
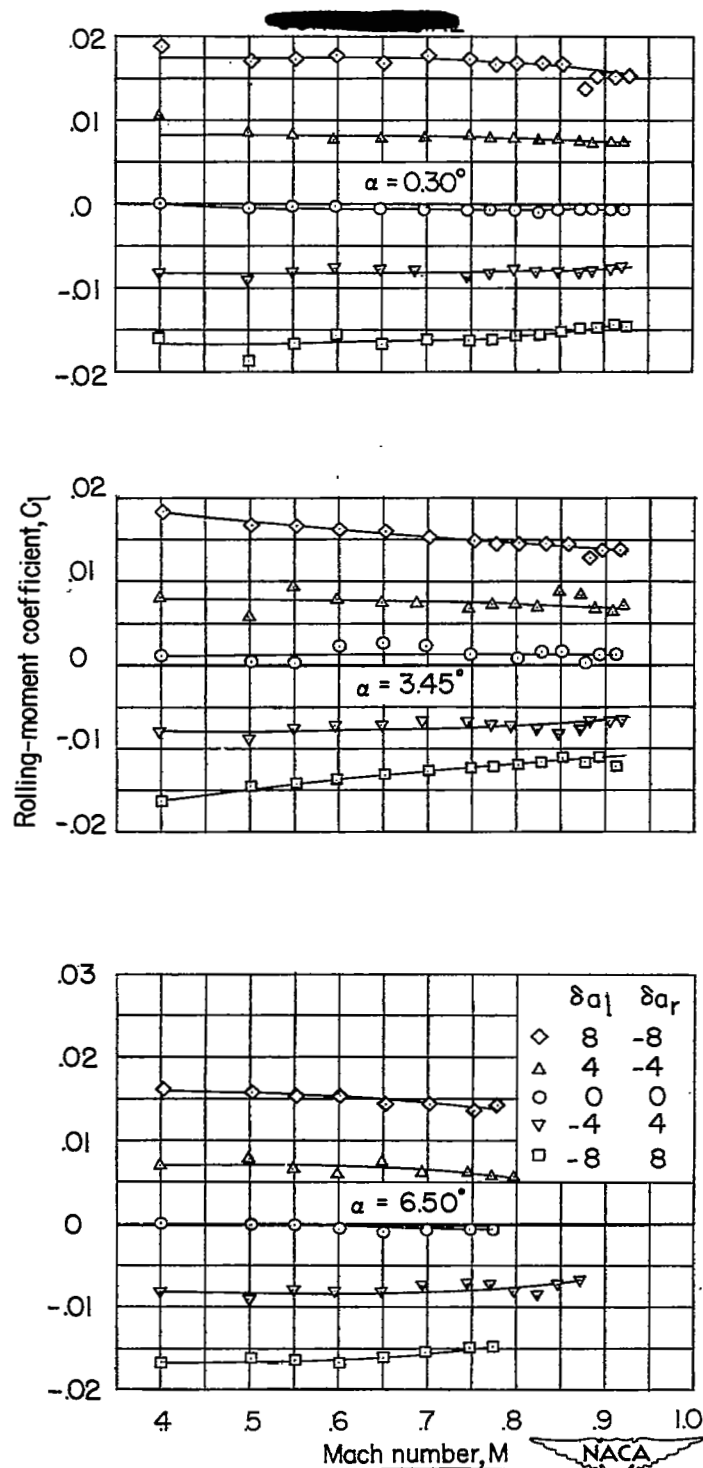
Figure 8.— The variation with Mach number of the rolling–moment
characteristics of a wing for various aileron deflections at
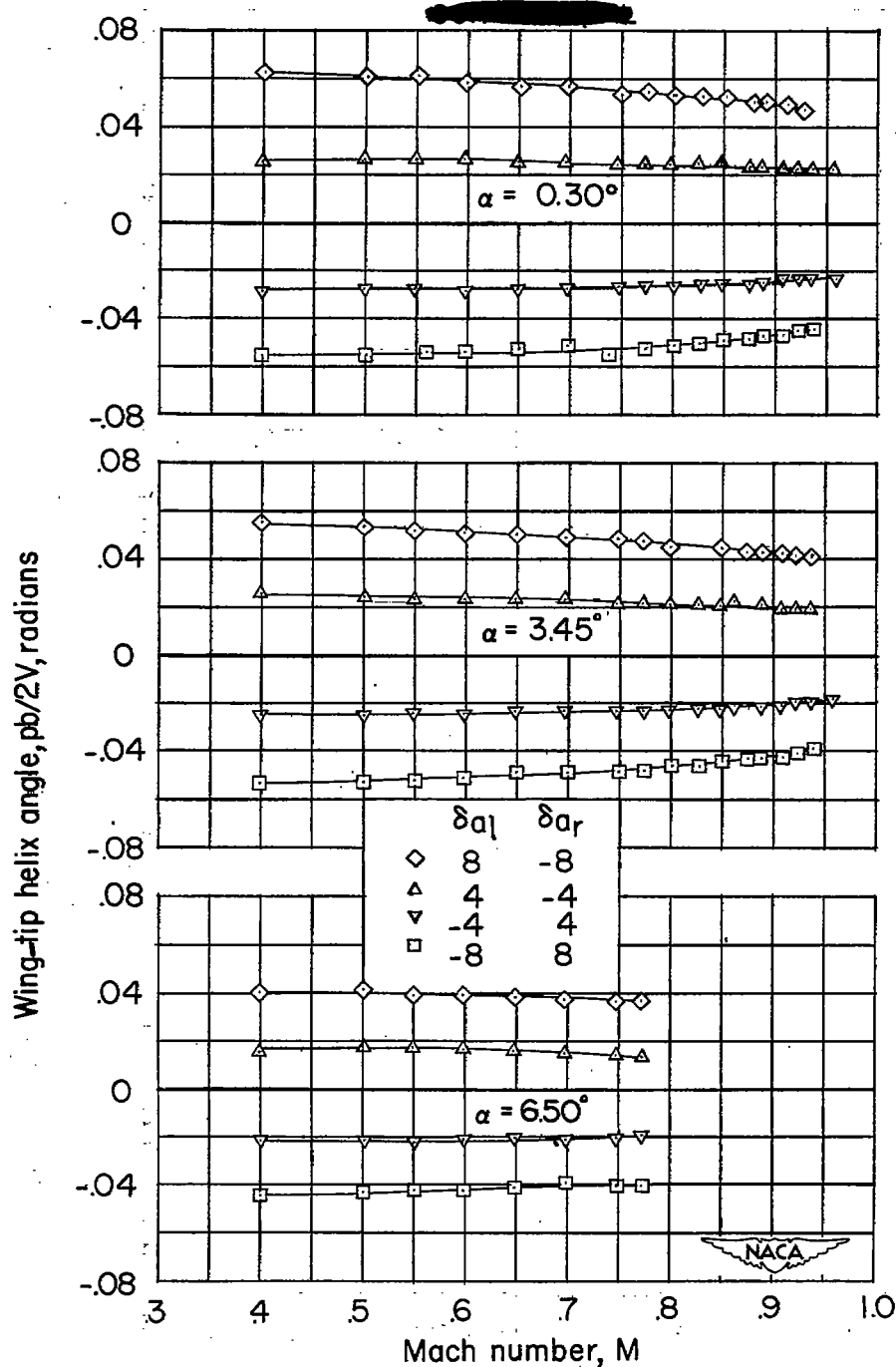several angles of attack. $\Lambda_{c/4} = 46.7°$.

Figure 9.— The variation with Mach number of the wing—tip helix angle $\frac{pb}{2V}$ for various aileron deflections at several angles of attack. $\Lambda_{c/4} = 3.6°$.
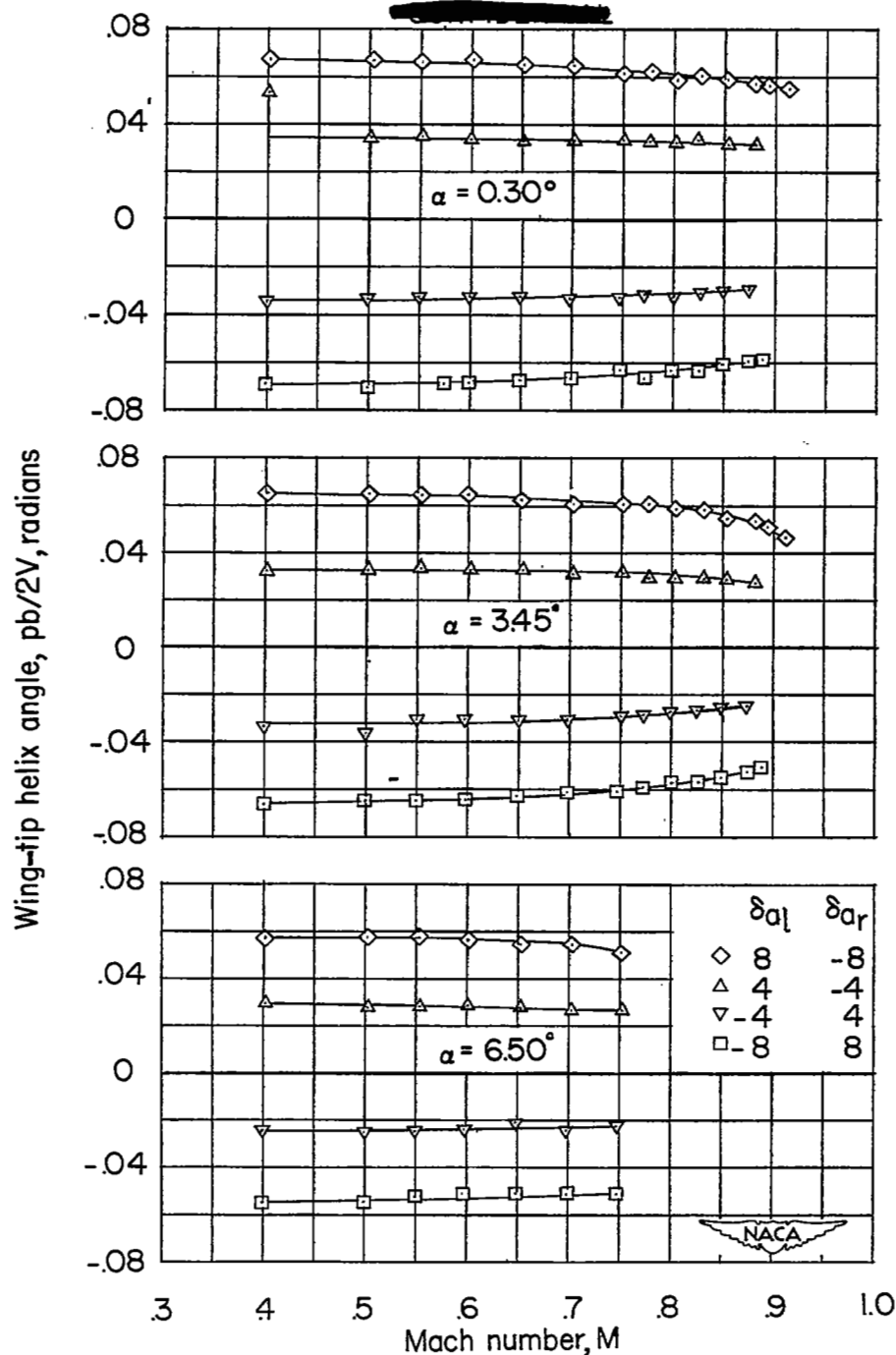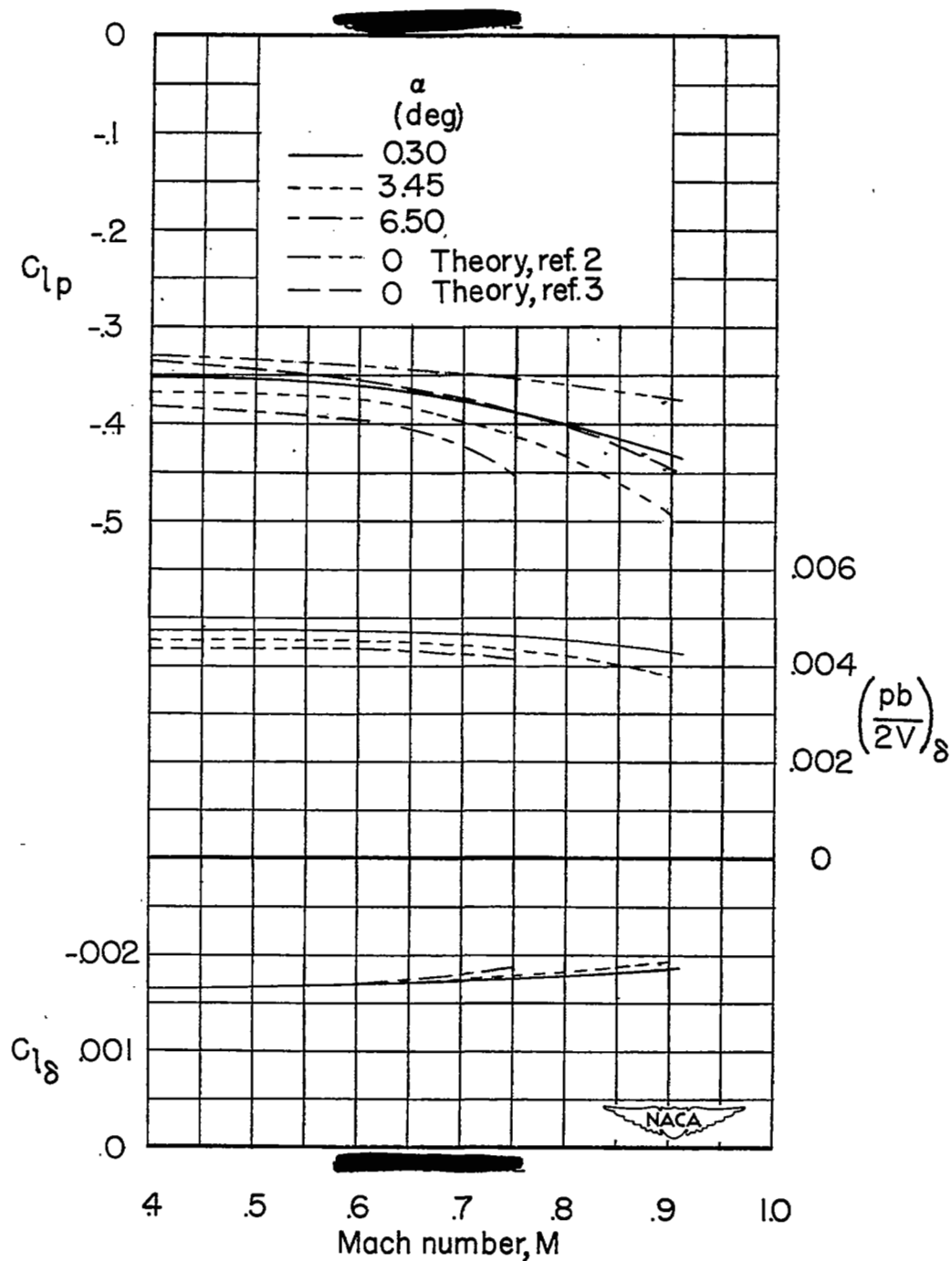
Figure 10.— The variation with Mach number of the wing—tip helix angle $\frac{pb}{2V}$ for various aileron deflections at several angles of attack. $\Lambda_{c}/_4 = 32.6°$.

Figure 11.— The variation with Mach number of the wing—tip helix angle $\frac{pb}{2V}$ for various aileron deflections at several angles of attack. $\Lambda_c/4 = 46.7°$.
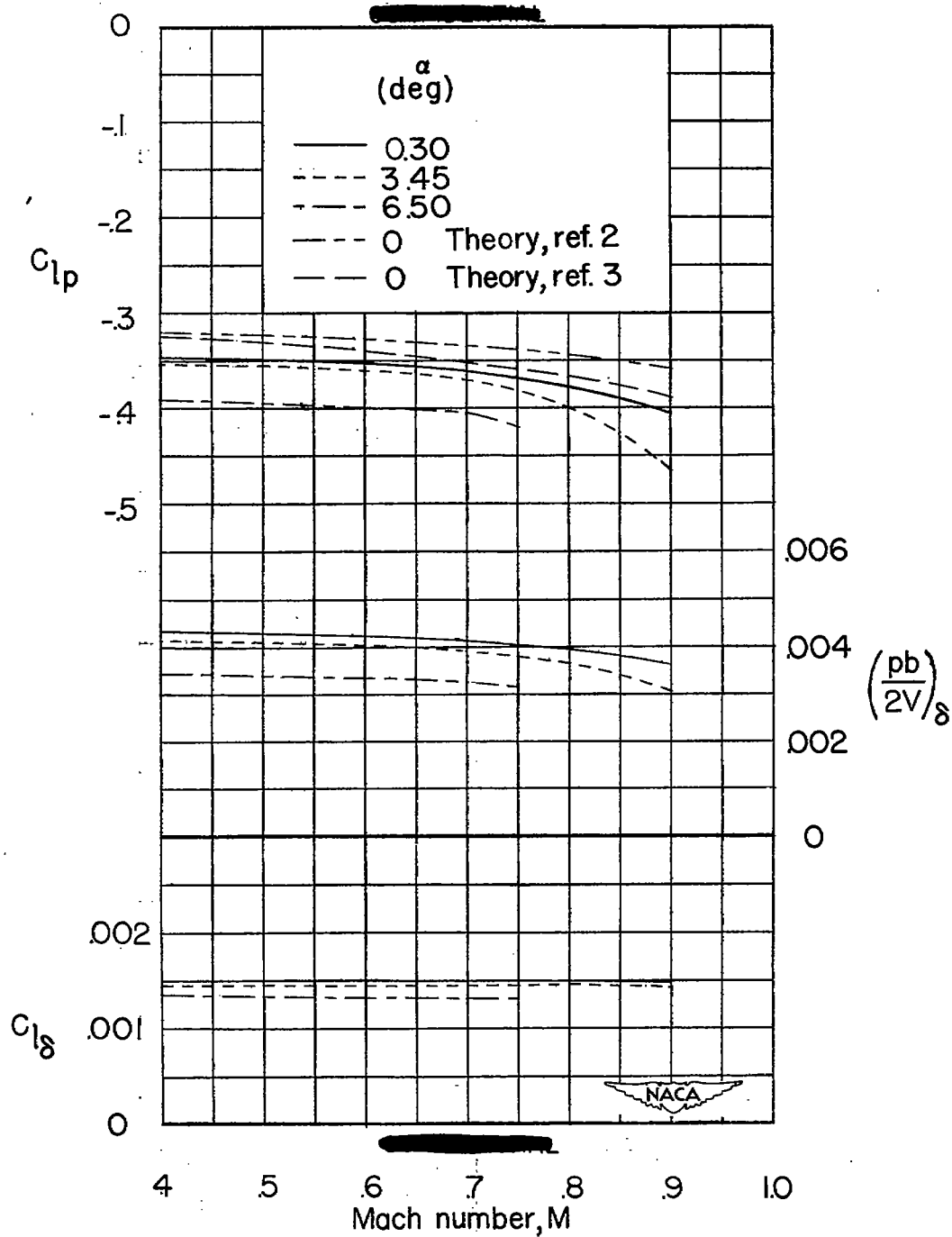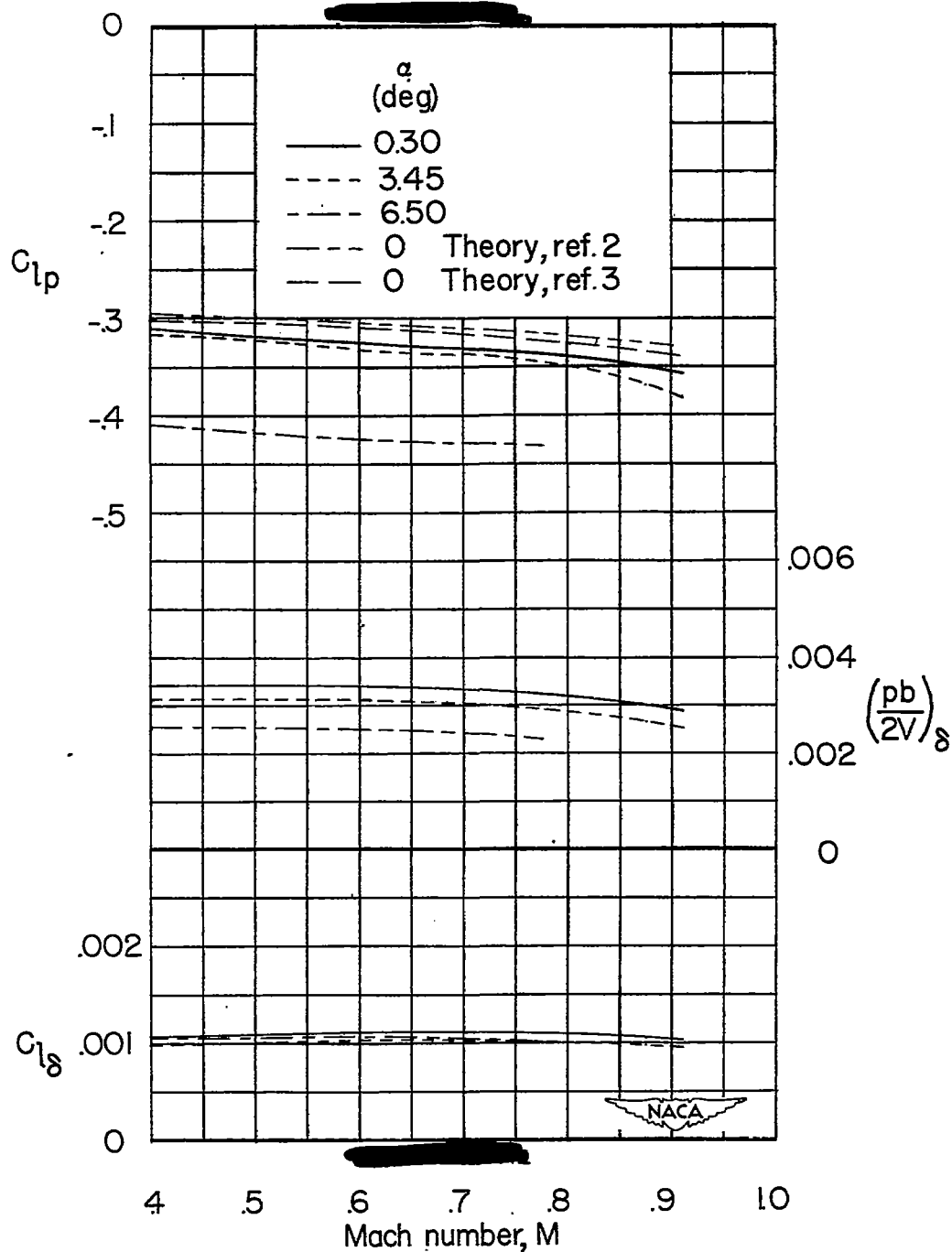
Figure 12.— The variation with Mach number of the parameters C_{l_p}, C_{l_δ}, and $\left(\frac{pb}{2V}\right)_\delta$ at several angles of attack for the 3.6° sweptback wing.

Figure 13.— The variation with Mach number of the parameters C_{l_p}, C_{l_δ}, and $\left(\frac{pb}{2V}\right)_\delta$ at several angles of attack for the 32.6° sweptback wing.

Figure 14.— The variation with Mach number of the parameters C_{l_p}, C_{l_δ}, and $\left(\frac{pb}{2V}\right)_\delta$ at several angles of attack for the 46.7° sweptback wing.
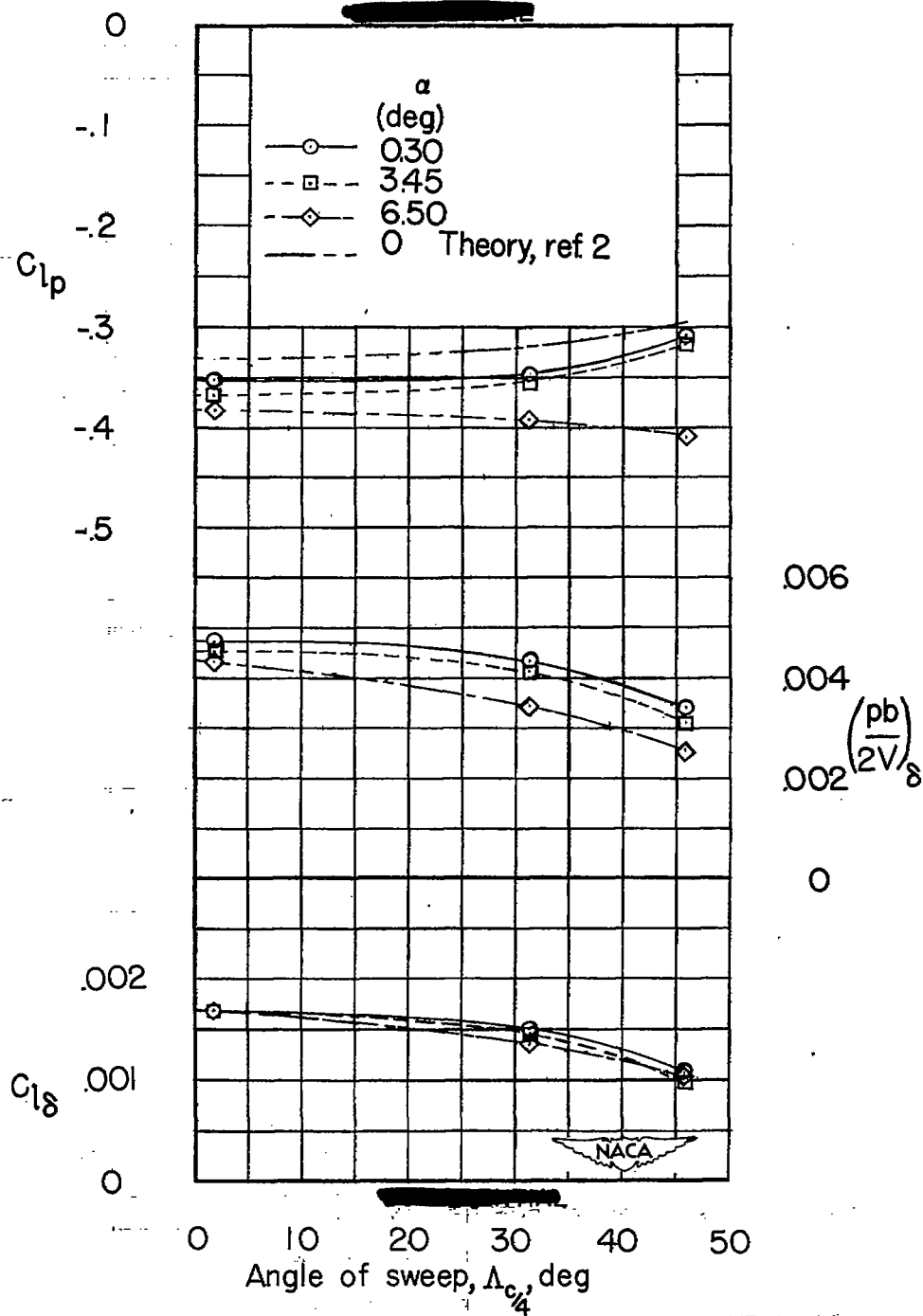
(a) $M = 0.40$.

Figure 15.— The effect of sweep angle on the parameters C_{l_p}, C_{l_δ},

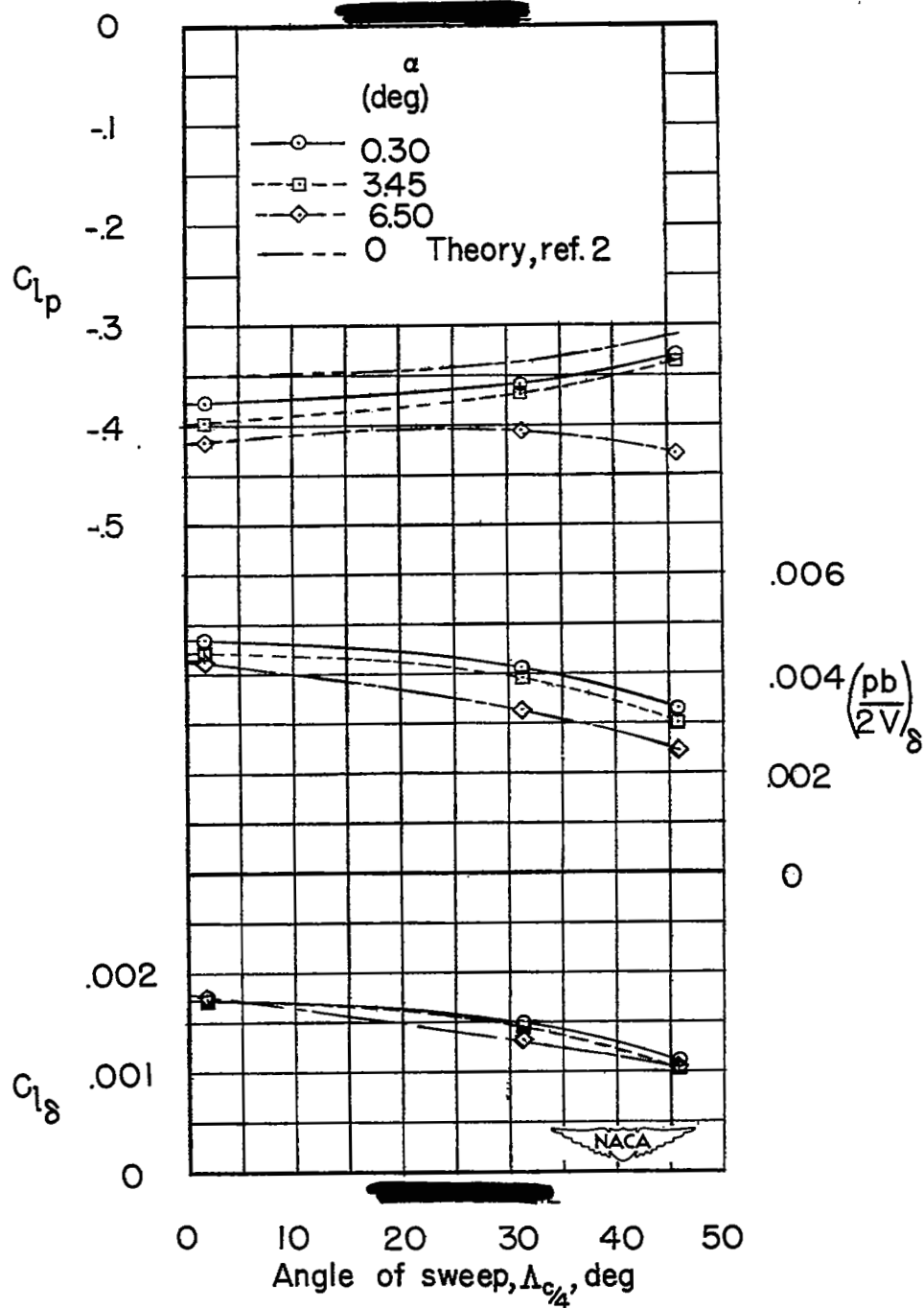and $\left(\frac{pb}{2V}\right)_\delta$ at several angles of attack and for various Mach numbers.

(b) M = 0.70.

Figure 15.— Continued.

Error

An error occurred while processing this page. See the system log for more details.